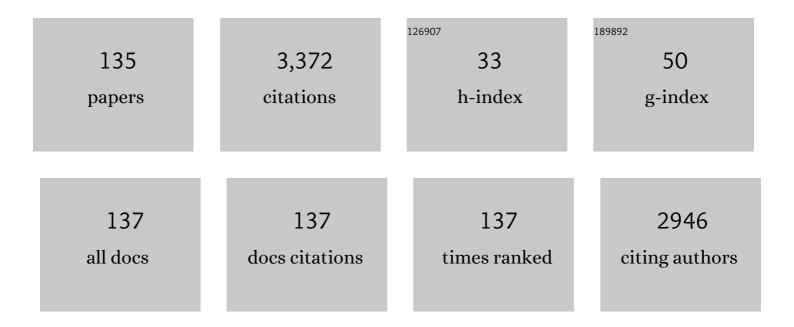
## **Didier Chicot**

List of Publications by Year in descending order

Source: https://exaly.com/author-pdf/4886710/publications.pdf Version: 2024-02-01



#	Article	IF	CITATIONS
1	Mechanical properties of magnetite (Fe3O4), hematite (α-Fe2O3) and goethite (α-FeO·OH) by instrumented indentation and molecular dynamics analysis. Materials Chemistry and Physics, 2011, 129, 862-870.	4.0	164
2	Absolute hardness of films and coatings. Thin Solid Films, 1995, 254, 123-130.	1.8	145
3	Apparent interface toughness of substrate and coating couples from indentation tests. Thin Solid Films, 1996, 283, 151-157.	1.8	122
4	Comparison of instrumented Knoop and Vickers hardness measurements on various soft materials and hard ceramics. Journal of the European Ceramic Society, 2007, 27, 1905-1911.	5.7	112
5	Effect of substrate roughness induced by grit blasting upon adhesion of WC-17% Co thermal sprayed coatings. Thin Solid Films, 2000, 377-378, 657-664.	1.8	82
6	Local mechanical properties of the 6061-T6 aluminium weld using micro-traction and instrumented indentation. European Journal of Mechanics, A/Solids, 2011, 30, 307-315.	3.7	81
7	Study of the mechanical behavior and corrosion resistance of hydroxyapatite sol–gel thin coatings on 316 L stainless steel pre-coated with titania film. Thin Solid Films, 2015, 593, 71-80.	1.8	81
8	Contribution of interferometry to Vickers indentation toughness determination of glass and ceramic glass. Optical Engineering, 2019, 58, 1.	1.0	78
9	Eddy currents and hardness testing for evaluation of steel decarburizing. NDT and E International, 2006, 39, 652-660.	3.7	65
10	Vickers Indentation Fracture (VIF) modeling to analyze multi-cracking toughness of titania, alumina and zirconia plasma sprayed coatings. Materials Science & Engineering A: Structural Materials: Properties, Microstructure and Processing, 2009, 527, 65-76.	5.6	61
11	Biocompatibility of sol-gel hydroxyapatite-titania composite and bilayer coatings. Materials Science and Engineering C, 2017, 72, 650-658.	7.3	61
12	Residual stresses and adhesion of thermal spray coatings. Surface Engineering, 2005, 21, 35-40.	2.2	60
13	Measurement of residual stress in thermal spray coatings by the incremental hole drilling method. Surface and Coatings Technology, 2006, 201, 2092-2098.	4.8	59
14	Hardness length-scale factor to model nano- and micro-indentation size effects. Materials Science & Engineering A: Structural Materials: Properties, Microstructure and Processing, 2009, 499, 454-461.	5.6	59
15	An experimental analysis and modeling of the work-softening transient due to dynamic recrystallization. International Journal of Plasticity, 2014, 54, 113-131.	8.8	58
16	Fatigue behavior of a 316L stainless steel coated with a DLC film deposited by PVD magnetron sputter ion plating. Materials Science & Engineering A: Structural Materials: Properties, Microstructure and Processing, 2010, 527, 498-508.	5.6	57
17	Comparison of conventional Knoop and Vickers hardness of ceramic materials. Journal of the European Ceramic Society, 2017, 37, 2531-2535.	5.7	57
18	Mechanical properties of conventional and nanostructured plasma sprayed alumina coatings. Mechanics of Materials, 2012, 53, 61-71.	3.2	51

#	Article	IF	CITATIONS
19	Fatigue and corrosion fatigue behavior of an AA6063-T6 aluminum alloy coated with a WC–10Co–4Cr alloy deposited by HVOF thermal spraying. Surface and Coatings Technology, 2008, 202, 4572-4577.	4.8	50
20	Role of residual stresses on interface toughness of thermally sprayed coatings. Thin Solid Films, 2002, 415, 143-150.	1.8	49
21	Mechanical properties of suspension plasma sprayed hydroxyapatite coatings submitted to simulated body fluid. Surface and Coatings Technology, 2010, 205, 954-960.	4.8	49
22	Influence of visco-elasto-plastic properties of magnetite on the elastic modulus: Multicyclic indentation and theoretical studies. Materials Chemistry and Physics, 2010, 119, 75-81.	4.0	47
23	New developments for fracture toughness determination by Vickers indentation. Materials Science and Technology, 2004, 20, 877-884.	1.6	42
24	A criterion to identify sinking-in and piling-up in indentation of materials. International Journal of Mechanical Sciences, 2015, 90, 145-150.	6.7	42
25	A contact area function for Berkovich nanoindentation: Application to hardness determination of a TiHfCN thin film. Thin Solid Films, 2014, 558, 259-266.	1.8	41
26	Mechanical tensile properties by spherical macroindentation using an indentation strain-hardening exponent. International Journal of Mechanical Sciences, 2013, 75, 257-264.	6.7	40
27	Influence of mechanical properties of tungsten carbide–cobalt thermal spray coatings on their solid particle erosion behaviour. Surface Engineering, 2012, 28, 237-243.	2.2	37
28	Influence of porosity on the mechanical properties of microporous β-TCP bioceramics by usual and instrumented Vickers microindentation. Journal of the European Ceramic Society, 2011, 31, 1361-1369.	5.7	36
29	Characterization of 100Cr6 lattice structures produced by robocasting. Materials and Design, 2017, 121, 345-354.	7.0	36
30	Part II: tribological performance of Cr3C2-25% NiCr reactive plasma sprayed coatings deposited at different pressures. Surface and Coatings Technology, 2001, 146-147, 563-570.	4.8	35
31	Depth-sensing indentation modeling for determination of Elastic modulus of thin films. Mechanics of Materials, 2010, 42, 166-174.	3.2	35
32	Analysis of the work-hardening behavior of C–Mn steels deformed under hot-working conditions. International Journal of Plasticity, 2013, 51, 145-160.	8.8	35
33	A model to determine the surface hardness of thin films from standard micro-indentation tests. Thin Solid Films, 2006, 497, 232-238.	1.8	34
34	Thin film hardness determination using indentation loading curve modelling. Thin Solid Films, 2010, 518, 5565-5571.	1.8	34
35	Characterization of expanded austenite developed on AISI 316L stainless steel by plasma carburization. Surface and Coatings Technology, 2010, 204, 3750-3759.	4.8	34
36	Corrosion behavior of Cr3C2–NiCr vacuum plasma sprayed coatings. Surface and Coatings Technology, 2008, 202, 4566-4571.	4.8	33

#	Article	IF	CITATIONS
37	Microstructure and adhesion of Cr3C2–NiCr vacuum plasma sprayed coatings. Surface and Coatings Technology, 2008, 202, 4406-4410.	4.8	31
38	Indentation tests to determine the fracture toughness of nickel phosphorus coatings. Surface and Coatings Technology, 2002, 155, 161-168.	4.8	30
39	Interface indentation test for the determination of adhesive properties of thermal sprayed coatings. Journal of Materials Science Letters, 1996, 15, 1377-1380.	0.5	29
40	Application of the interfacial indentation test for adhesion toughness determination. Surface and Coatings Technology, 2005, 200, 174-177.	4.8	29
41	Effect of substrate roughness on the fatigue behavior of a SAE 1045 steel coated with a WC–10Co–4Cr cermet, deposited by HVOF thermal spray. Materials Science & Engineering A: Structural Materials: Properties, Microstructure and Processing, 2010, 527, 6551-6561.	5.6	29
42	Work-of-indentation coupled to contact stiffness for calculating elastic modulus by instrumented indentation. Mechanics of Materials, 2016, 94, 170-179.	3.2	29
43	Elastic properties determination from indentation tests. Surface and Coatings Technology, 1996, 81, 269-274.	4.8	28
44	Hardness measurements of Ti and TiC multilayers: a model. Thin Solid Films, 2000, 359, 228-235.	1.8	27
45	Fatigue behavior of AA7075-T6 aluminum alloy coated with a WC–10Co–4Cr cermet by HVOF thermal spray. Surface and Coatings Technology, 2013, 220, 122-130.	4.8	27
46	Modeling of elastic modulus and hardness determination by indentation of porous yttria stabilized zirconia coatings. Surface and Coatings Technology, 2013, 220, 131-139.	4.8	27
47	Influence of sinking-in and piling-up on the mechanical properties determination by indentation: A case study on rolled and DMLS stainless steel. Materials Science & Engineering A: Structural Materials: Properties, Microstructure and Processing, 2013, 576, 126-133.	5.6	26
48	Models for hardness and adhesion of coatings. Surface Engineering, 1999, 15, 447-453.	2.2	25
49	Wear Behaviour of Silicon Carbide/Electroless Nickel Composite Coatings at High Temperature. Surface Engineering, 2002, 18, 265-269.	2.2	25
50	Adhesion tests for thermal spray coatings: Correlation of bond strength and interfacial toughness. Surface Engineering, 2007, 23, 279-283.	2.2	25
51	Microstructural and mechanical characterization of Ni-base thermal spray coatings deposited by HVOF. Surface and Coatings Technology, 2008, 202, 4552-4559.	4.8	25
52	Influence of tip defect and indenter shape on the mechanical properties determination by indentation of a TiB2–60%B4C ceramic composite. International Journal of Refractory Metals and Hard Materials, 2013, 38, 102-110.	3.8	24
53	Analysis of indentation size effect in copper and its alloys. Materials Science and Technology, 2013, 29, 868-876.	1.6	24
54	Constitutive description for the design of hot-working operations of a 20MnCr5 steel grade. Materials & Design, 2014, 62, 255-264.	5.1	24

4

#	Article	IF	CITATIONS
55	Fatigue behavior of a SAE 1045 steel coated with Colmonoy 88 alloy deposited by HVOF thermal spray. Surface and Coatings Technology, 2010, 205, 1119-1126.	4.8	23
56	Cr2C3–NiCr VPS thermal spray coatings as candidate for chromium replacement. Surface and Coatings Technology, 2013, 220, 225-231.	4.8	23
57	Effect of thermal treatments on adhesive properties of a NiCr thermal sprayed coating. Thin Solid Films, 2000, 377-378, 681-686.	1.8	22
58	Improvement in depth-sensing indentation to calculate the universal hardness on the entire loading curve. Mechanics of Materials, 2008, 40, 171-182.	3.2	22
59	A new approach of the Oliver and Pharr model to fit the unloading curve from instrumented indentation testing. Journal of Materials Research, 2017, 32, 2230-2240.	2.6	22
60	Diamond-like carbon film deposited on nitrided 316L stainless steel substrate: A hardness depth-profile modeling. Diamond and Related Materials, 2011, 20, 1344-1352.	3.9	21
61	Reliability analysis of solder joints due to creep and fatigue in microelectronic packaging using microindentation technique. Microelectronics Reliability, 2013, 53, 761-766.	1.7	21
62	A multilayer coating with optimized properties for corrosion protection of Al. Journal of Materials Chemistry A, 2015, 3, 15977-15985.	10.3	21
63	Fatigue performance of a SAE 1045 steel coated with a Colmonoy 88 alloy deposited by HVOF thermal spraying. Surface and Coatings Technology, 2006, 201, 2038-2045.	4.8	20
64	Fatigue behavior of a structural steel coated with a WC–10Co–4Cr/Colmonoy 88 deposit by HVOF thermal spraying. Surface and Coatings Technology, 2013, 220, 248-256.	4.8	20
65	Hardness of thermal sprayed coatings: Relevance of the scale of measurement. Surface and Coatings Technology, 2015, 268, 173-179.	4.8	20
66	Indentation creep analysis of T22 and T91 chromium based steels. Materials Science & Engineering A: Structural Materials: Properties, Microstructure and Processing, 2016, 652, 315-324.	5.6	20
67	Mechanical characterization of brittle materials using instrumented indentation with Knoop indenter. Mechanics of Materials, 2017, 108, 58-67.	3.2	19
68	A model for hardness determination of thin coatings from standard micro-indentation tests. Surface and Coatings Technology, 2005, 200, 886-889.	4.8	18
69	Interpretation of instrumented hardness measurements on stainless steel with different surface preparations. Surface Engineering, 2007, 23, 32-39.	2.2	18
70	Strain gradient plasticity to study hardness behavior of magnetite (Fe <sub>3</sub> O <sub>4</sub> ) under multicyclic indentation. Journal of Materials Research, 2009, 24, 749-759.	2.6	18
71	Adhesion of YSZ suspension plasma-sprayed coating on smooth and thin substrates. Surface and Coatings Technology, 2010, 205, 999-1003.	4.8	17
72	An analysis of the elastic properties of a porous aluminium oxide film by means of indentation techniques. Materials Science & Engineering A: Structural Materials: Properties, Microstructure and Processing, 2013, 585, 155-164.	5.6	15

#	Article	IF	CITATIONS
73	Mechanical properties by instrumented indentation of solution precursor plasma sprayed hydroxyapatite coatings: Analysis of microstructural effect. Surface and Coatings Technology, 2016, 298, 93-102.	4.8	15
74	Hydroxyapatite-TiO2-SiO2-Coated 316L Stainless Steel for Biomedical Application. Metallurgical and Materials Transactions A: Physical Metallurgy and Materials Science, 2017, 48, 3570-3582.	2.2	15
75	Nanoindentation Analysis of Friction Stir Welded 6061-T6 Al Alloy in As-Weld and Post Weld Heat Treatment. Physics of Metals and Metallography, 2019, 120, 483-491.	1.0	14
76	Effect of some thermal treatments on interface adhesion toughness of various thick thermal spray coatings. Surface Engineering, 2006, 22, 390-398.	2.2	13
77	Elastic modulus of TiHfCN thin films by instrumented indentation. Thin Solid Films, 2012, 522, 304-313.	1.8	13
78	Titanium carbide films obtained by conversion of sputtered titanium on high carbon steel. Surface and Coatings Technology, 2006, 200, 5447-5454.	4.8	11
79	Analysis of data from various indentation techniques for thin films intrinsic hardness modelling. Thin Solid Films, 2008, 516, 1964-1971.	1.8	11
80	Mechanical Properties of Yttria- and Ceria-Stabilized Zirconia Coatings Obtained by Suspension Plasma Spraying. Journal of Thermal Spray Technology, 2013, 22, 125-130.	3.1	11
81	Constitutive description of Fe–Mn23–C0.6 steel deformed under hot-working conditions. International Journal of Mechanical Sciences, 2015, 99, 143-153.	6.7	11
82	Morphological and Mechanical Properties of Hydroxyapatite Bilayer Coatings Deposited on 316L SS by Sol–Gel Method. Metallurgical and Materials Transactions B: Process Metallurgy and Materials Processing Science, 2015, 46, 2340-2347.	2.1	11
83	Characterization of brazed joints by electrical resistance spot brazing with Ni-based amorphous self-flux alloys. Journal of Manufacturing Processes, 2019, 37, 617-627.	5.9	11
84	Tribological study of WC produced by plasma pressure compaction. International Journal of Refractory Metals and Hard Materials, 2006, 24, 183-188.	3.8	10
85	Correlation between yield stress and hardness of nickel–silicon–boron-based alloys by nanoindentation. Materials Science & Engineering A: Structural Materials: Properties, Microstructure and Processing, 2014, 605, 294-300.	5.6	10
86	Influence of hydrogen contamination on the tensile behavior of a plasma ion nitrided steel. Materials Science & Engineering A: Structural Materials: Properties, Microstructure and Processing, 2000, 282, 203-212.	5.6	9
87	Sliding Wear Response of Nanostructured YSZ Suspension Plasma-Sprayed Coating. Journal of Thermal Spray Technology, 2014, 23, 1350-1361.	3.1	9
88	Mechanical properties of thermally sprayed porous alumina coating by Vickers and Knoop indentation. Ceramics International, 2020, 46, 19843-19851.	4.8	9
89	Estimation du module d'Young par analyse de la géométrie de l'empreinte résiduelle après indenta Vickers. Revue De Metallurgie, 1995, 92, 635-643.	ition 0.3	8
90	Mechanical properties of WC coatings evaluated using instrumented indentation technique. Surface Engineering, 2014, 30, 498-510.	2.2	8

#	Article	IF	CITATIONS
91	Role of grain boundaries and micro-defects on the mechanical response of a crystalline rock at multiscale. International Journal of Rock Mechanics and Minings Sciences, 2014, 71, 429-441.	5.8	8
92	Mechanical characterization by multiscale instrumented indentation of highly heterogeneous materials for braking applications. Journal of Materials Science, 2019, 54, 4647-4670.	3.7	8
93	Model to determine the depth of a diffusion layer by normal indentations to the surface. Surface and Coatings Technology, 2008, 202, 3419-3426.	4.8	7
94	Comments on the paper "Modification of composite hardness models to incorporate indentation size effects in thin filmsâ€; D. Beegan, S. Chowdhury and M.T. Laugier, Thin Solid Films 516 (2008), 3813–3817. Thin Solid Films, 2010, 518, 2097-2101.	1.8	7
95	Combined loading and failure analysis of lead-free solder joints due to creep and fatigue phenomena. Soldering and Surface Mount Technology, 2014, 26, 22-26.	1.5	7
96	Some improvements for determining the hardness of homogeneous materials from the work-of-indentation. International Journal of Mechanical Sciences, 2016, 105, 279-290.	6.7	7
97	Prediction of hardness–depth profile from indentations at surface of materials. Surface Engineering, 2009, 25, 93-96.	2.2	6
98	Indentation size effect of cortical bones submitted to different soft tissue removals. Journal of the Mechanical Behavior of Biomedical Materials, 2013, 20, 338-346.	3.1	6
99	Structure and hardness of diamond films deposited on WC–Co by CVD technique. Surface and Coatings Technology, 2013, 227, 70-74.	4.8	6
100	Modeling of very thin aluminum nitride film mechanical properties from nanoindentation measurements. Thin Solid Films, 2015, 594, 129-137.	1.8	6
101	Hardness evaluation from a bilayer coating system of Ni-P deposited on carbon steel plates by multicycle indentation tests. Surface and Coatings Technology, 2018, 334, 410-419.	4.8	6
102	Virtual machine concept applied to uncertainties estimation in instrumented indentation testing. Journal of Materials Research, 2019, 34, 2501-2516.	2.6	6
103	Indentation instrumentée multi-échelles appliquée à l'étude des matériaux massifs métalliques. Materiaux Et Techniques, 2017, 105, 104.	0.9	6
104	A Damage Criterion to Predict the Fatigue Life of Steel Pipelines Based on Indentation Measurements. Journal of Offshore Mechanics and Arctic Engineering, 2021, 143, .	1.2	6
105	Sliding wear of a-C:H coatings against alumina in corrosive media. Diamond and Related Materials, 2013, 38, 139-147.	3.9	5
106	Annealing study of thin chromium layers on cemented steel substrates. Surface and Coatings Technology, 2013, 227, 65-69.	4.8	5
107	Microstructure analysis and mechanical properties by instrumented indentation of Charonia Lampas Lampas shell. Journal of the Mechanical Behavior of Biomedical Materials, 2019, 89, 114-121.	3.1	5
108	Instrumented indentation study of slag in view of a better valorization. Construction and Building Materials, 2019, 199, 349-358.	7.2	5

#	Article	IF	CITATIONS
109	Adhesive and cohesive properties of nanostructured ZrO2 coatings by the original Vickers Indentation Cracking technique. Thin Solid Films, 2011, 519, 7789-7795.	1.8	4
110	Mechanical properties of an Al91–Mn6–Nd3 nanostructured alloy. Materials Science & Engineering A: Structural Materials: Properties, Microstructure and Processing, 2011, 528, 7041-7051.	5.6	4
111	Hardness-load modelling applied to multilayer galvanised coatings. Surface Engineering, 2016, 32, 194-200.	2.2	4
112	High Cycle Fatigue Damage Evaluation of Steel Pipelines Based on Microhardness Changes During Cyclic Loads. , 2017, , .		4
113	Analyzing the nanoindentation response of carbon black filled elastomers. Journal of Applied Polymer Science, 2021, 138, 50697.	2.6	4
114	Role of hydrogen on adhesion of NiCr thermal sprayed coatings. Thin Solid Films, 2000, 377-378, 675-680.	1.8	3
115	Effect of impregnation solutions on the synthesis of Ni-Cu/Al <sub>2</sub> O <sub>3</sub> catalyst to obtain carbon nanofibers. Materials Research Express, 2018, 5, 125010.	1.6	3
116	Fatigue Life Prediction of Steel Pipelines Based on X-ray Diffraction Analyses. Journal of Materials Engineering and Performance, 2022, 31, 801-813.	2.5	3
117	Indentation : fondamentaux et d $ ilde{A}$ $ ilde{C}$ veloppements. Materiaux Et Techniques, 2017, 105, 101.	0.9	3
118	Multiscale study of cold-rolling deformation on mechanical and corrosion behaviors of AA2024-T4 aluminum alloy. Journal of the Indian Chemical Society, 2022, 99, 100307.	2.8	3
119	Hydrogen Diffusion in Plasma Ion Nitrided Steel. Defect and Diffusion Forum, 1997, 143-147, 939-944.	0.4	2
120	Maintenance of solder joints on the strength of simultaneously acting creep and fatigue phenomena by using microindentation technique. , 2013, , .		2
121	Role of plastic deformation on the efficiency of a nitriding treatment: modelling of the hardness-depth profile. International Journal of Microstructure and Materials Properties, 2013, 8, 155.	0.1	2
122	High Cycle Fatigue Damage Evaluation of Steel Pipelines Based on Microhardness Changes During Cyclic Loads: Part II. , 2018, , .		2
123	Quantitative evaluation of interfacial adhesion between steel reinforcements and self-compacting concretes, in steel/concrete composites, by indentation tests. Composite Interfaces, 2020, 27, 307-326.	2.3	2
124	Effet de l'addition de TiB2 sur les propriétés mécaniques et tribologiques de revêtements NiCrBSi déposés par projection thermique. Materiaux Et Techniques, 2018, 106, 202.	0.9	2
125	Interfacial Indentation Test for the Study of Reinforcement bar/concrete matrix Adhesion i n High Performance Self Compacting Concretes. Journal of Materials and Environmental Science, 2018, 9, 189-200.	0.5	2
126	Microhardness and spectroscopy studies of surface modification of titanium alloys by melted metaphosphates. Thin Solid Films, 1994, 241, 230-233.	1.8	1

#	Article	IF	CITATIONS
127	Experimental system for analysing the combined loading and failure modes of solder joints in electronic packaging. , 2012, , .		1
128	Conversion treatment of thin titanium layer deposited on carbon steel. Journal of Physics: Conference Series, 2018, 1033, 012010.	0.4	1
129	Un critere simple d'identification du mode de déformation par indentation. Materiaux Et Techniques, 2015, 103, 603.	0.9	1
130	Étude des transformations microstructurales survenant lors deÂl'endommagement par frottement sec d'un couple fonte/acierA study of microstructural transformations occurring during the deterioration by dry friction of an iron/steel pair. Mecanique Et Industries, 2002, 3, 237-243.	0.2	0
131	Eddy currents to control steel decarburising. Surface Engineering, 2007, 23, 273-278.	2.2	0
132	WÅ,aÅ›ciwoÅ›ci mechaniczne powÅ,ok hydroksyapatytu natryskiwanych plazmowo z zawiesin. PrzeglÄd Spawalnictwa, 2015, 84, .	0.5	0
133	Propriétés mécaniques par indentation d'un film mince nanometrique de nitrure d'aluminium. Materiaux Et Techniques, 2015, 103, 605.	0.9	0
134	Fluage et relaxation par indentation d'aciers au chrome. Materiaux Et Techniques, 2017, 105, 103.	0.9	0
135	Structure and microstructure study of Charonia lampas lampas shell. Acta Crystallographica Section A: Foundations and Advances, 2019, 75, e200-e200.	0.1	0